AD-A086 004 ANALYTIC SCIENCES CORP READING MA F/G 17/7
DESIGN AND CALIBRATION OF A GRID PREDICTION ALGORITHM FOR THE S--ETC(U)
MAR 78 R S WARREN, R R GUPTA, R D HEALY DOT-CG-81-77-1785
UNCLASSIFIED TASC-TIM-1119-2 USCG-D-32-80 NL

2 OF 2
AD
A086004

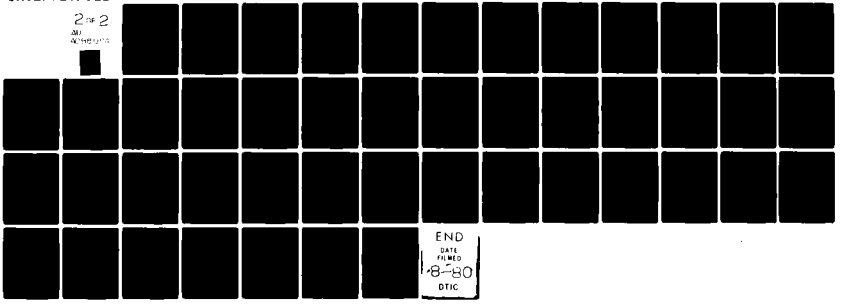

END
DATE FILMED
8-80
DTIC

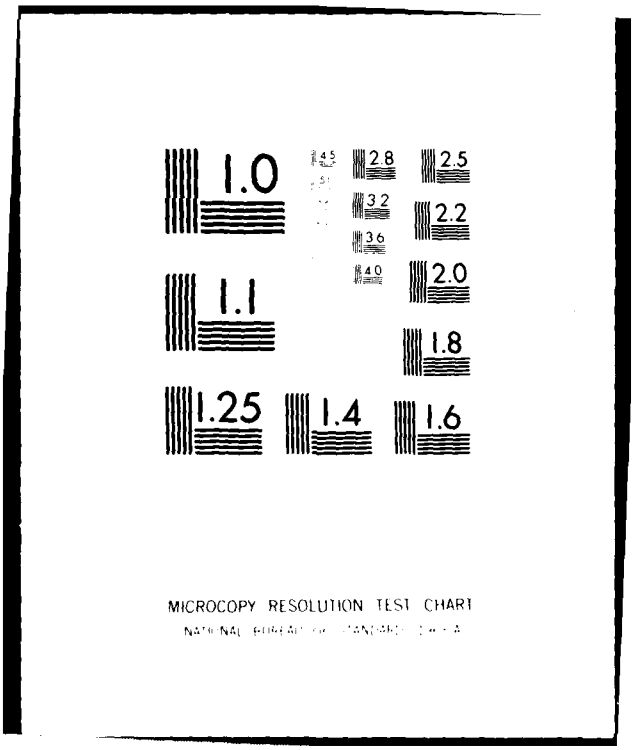
1.0
1.1
1.25
1.4
1.6
1.8
2.0
2.2
2.5
2.8
3.2
3.6
4.0
4.5
MICROCOPY RESOLUTION TEST CHART

R-32763

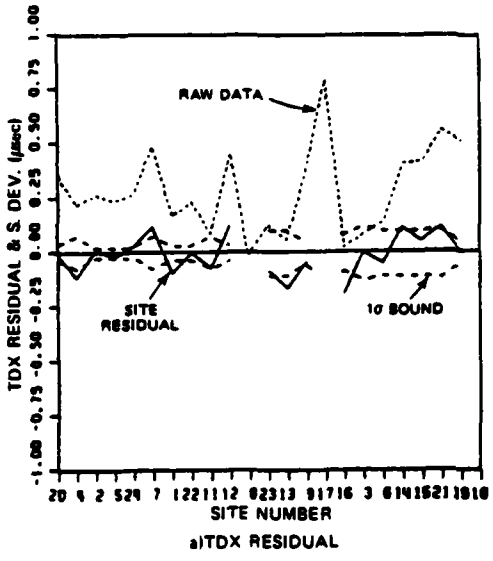

a)TDX RESIDUAL

R-32764

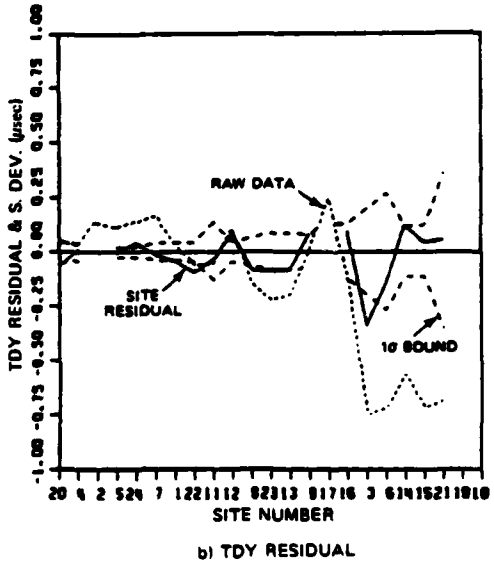

b) TDY RESIDUAL

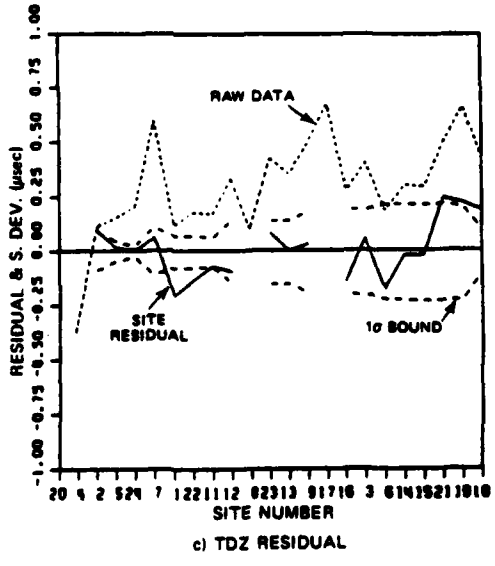

c) TDZ RESIDUAL

Figure 7.4-4 TD Residuals With RB Model, Weighted Noise (20 nsec/TD at SAM and Scaled as Function of Distance From SAM)

TABLE 7.4-1
RESIDUAL TD ERROR STATISTICS FOR ENSEMBLE OF SITES

MEASUREMENT NOISE MODEL	STATISTIC	MODEL R			MODEL RB		
		TDX (nsec)	TDY (nsec)	TDZ (nsec)	TDX (nsec)	TDY (nsec)	TDZ (nsec)
Uniform	Mean	0	0	0	0	0	0
	Std. Deviation	99	111	95	98	82	117
Weighted	Mean	8	-42	10	-12	-10	-11
	Std. Deviation	116	113	103	91	124	129

TABLE 7.4-2
STATISTICS OF EDITED RAW* DATA TD RESIDUALS

STATISTIC	TD RESIDUAL (nsec)		
	TDX	TDY	TDZ
Mean	265	-67	347
Std. Deviation	319	368	369
RMS	415	374	507

*Raw data values based on assumption of velocity of light in air = 983.2444 ft/sec

raw data given in Table 7.4-2 shows a factor of three or more reduction in the error after calibration. The uniform noise model results in an unbiased estimate (zero mean) whereas the residuals with the weighted noise model exhibit a non-zero mean. This small non-zero mean is associated with the fact that the weighted noise model causes the calibration algorithm to place more emphasis on data from collection sites near the SAM site. Consequently, the resulting difference between the predicted and measured TDs at the SAM site are smaller with the weighted noise model, than with the uniform noise model as illustrated in Table 7.4-3.

TABLE 7.4-3
TD RESIDUALS AT SAM SITE

MEASUREMENT NOISE MODEL	MODEL R			MODEL RB		
	TDX (nsec)	TDY (nsec)	TDZ (nsec)	TDX (nsec)	TDY (nsec)	TDZ (nsec)
Uniform	26	157	18	49	69	17
Weighted	7	67	10	25	43	6

Substantial reduction in the SAM site TDY residual is provided by the RB model compared to the R model, when the uniform noise model is employed. However, both grid prediction models provide about the same residual errors when the weighted noise model is employed.

Although both calibration models yield nearly the same performance, the RB model appears to have a slightly better overall performance. Therefore, the RB model was selected to provide the final grid calibration results and to produce the required TD charts (Section 8). The detailed grid prediction algorithms associated with both models calibrated using the weighted noise model are given in Appendix A.

Additional testing of the RB model was also performed to evaluate the grid prediction error at collection sites which are not included in the data base used to calibrate the algorithm. A number of different subsets of the data base were formed by eliminating one or more collection sites, recalibrating the algorithm with the remaining sites and predicting the TDs at the sites eliminated from the data base. The overall performance statistics were essentially equivalent to the results given in Table 7.4-1 for all of these tests.

7.5 PREDICTED USER POSITION ERROR

This section presents the predicted position error performance of the St. Marys River TD grid charted with the calibrated range and bearing-dependent model selected in Section 7.4. The calibrated model coefficients are given in Appendix A and the position error computation algorithm is presented in Appendix B. Predicted user position errors at the downbound and upbound river waypoints for assumed user receiver noise (1σ) levels of 10, 50 and 100 nsec/TD are also given in Appendix B.

An example of the expected minimum 2d rms (defined in Appendix B) user position error for a perfect receiver (i.e., zero receiver noise) at the downbound waypoints is illustrated in Fig. 7.5-1. The minimum waypoint error corresponds to the station combination (or TD pair) which yields the smallest waypoint error, out of the three available combinations, to obtain a waypoint position fix. For the downbound waypoint errors shown in Fig. 7.5-1, the minimum error station combination is MXZ for the waypoint A through M and then changes to MXY for the waypoints T through II.

Figure 7.5-1 shows the expected waypoint errors with and without "assumed temporal grid instability". The predicted user error curve associated with residual grid prediction error (i.e., no temporal grid instability) shows the expected position errors if the propagation conditions across the chain exactly match the average conditions embodied in the calibrated spatial-area TD grid prediction model. However, because of suspected temporal variations in the grid, the position error will be larger than the residual grid prediction error with no temporal variations (i.e., no temporal grid instability). The error curve with assumed grid instability shows the expected

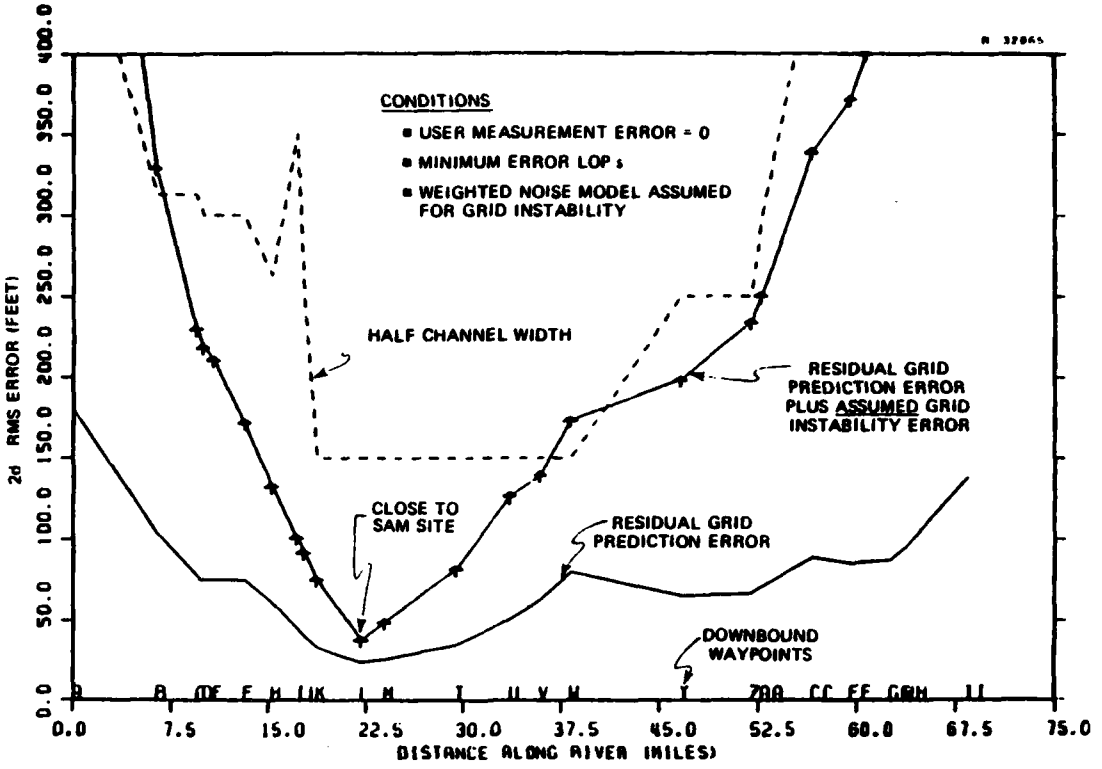

Figure 7.5-1 Predicted 2d RMS Downbound Waypoint Error

position errors if the chain has the same average properties that existed during model calibration and temporal variations which are consistent with the weighted measurement noise model. At waypoint L (close to the SAM site where grid instability errors are zero), both error curves (i.e., with and without the grid instability) have minimum errors of 40 ft and 30 ft, respectively. For increasing waypoint distances from the SAM site, the error increases much more rapidly with assumed grid instability than without the grid instability. Largest waypoint error occurs at waypoint A because of GDOP effects.

The assumed error due to grid instability is arrived at on an ad hoc basis; it is based on a very limited number of observations. It represents a "best engineering estimate" at this time and probably represents a worst-case error for

the region. The actual grid prediction error is felt to lie somewhere between the two error bounds shown in Fig. 7.5-1. If temporal data is collected and incorporated as a correction to the grid prediction algorithm, the user error will tend to approach the residual grid prediction error bound.

If the navigation channel is rather straight and narrow, a user may be more interested in cross-channel error than along-channel error or 2d rms error. Figure 7.5-2 shows the predicted 2σ cross-channel error at the downbound river waypoints for the same transmitting station combination that yielded the minimum 2d rms waypoint error (Fig. 7.5-1). Compared to the 2d rms error (Fig. 7.5-1), the 2σ cross-channel error component (Fig. 7.5-2) is especially small in the Neebish Channel and at the two extremes of the river.

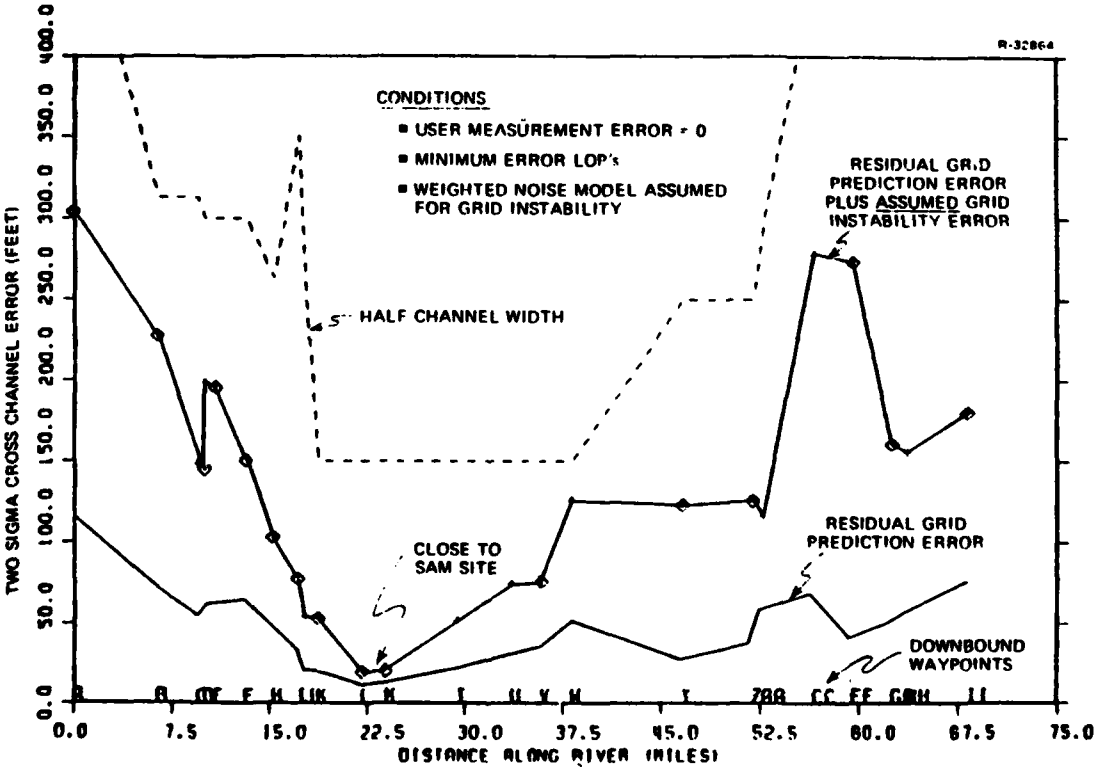

Figure 7.5-2 Predicted 2σ Cross-Channel Downbound Waypoint Error

8. CHART PRODUCTION

8.1 INTRODUCTION

As part of this effort, TASC produced three drawings of the St. Marys River to the size and scale of the Lake Survey Charts. Each drawing contained:

- Reference marks
- Approximate coastal outlines
- River channel centerlines
- Contours of constant Loran-C time differences.

Each drawing uses the same projection as the corresponding Lake Survey Chart. Reference marks were computed using the mathematical projection. Coastal outlines were transferred from the Lake Survey Charts using a digitizer and unitary transformation. The channel centerlines were plotted using the transformation described in Section 5.4. Time difference contours were plotted using the calibrated RB model described in Section 7.4.2 and Appendix A.

8.2 SOFTWARE

The software used to produce the charts can be placed into three categories:

- Coordinate transformations
- Contour generation
- Plotting.

These categories are representative of the process involved, but data sets were not processed sequentially through the categories.

The coordinate transformation software modules include POLYCON, POLYSEC, WPLOAD and FIXLS. POLYCON is the subroutine that computes the polyconic projection. Reference marks for each chart were processed using the central meridian data supplied in Table 5.2-1. Although the TASC coordinate system is a polyconic projection, it does not correspond to the projection used in Chart Nos. 61 and 63. (The central meridian of the TASC coordinate system was chosen to correspond to Lake Survey Chart No. 62.) Subroutine POLYSEC is used to correct all data supplied in TASC coordinates for the difference in projection between the TASC grid and Chart Nos. 61 and 63. Subroutine WPLOAD is used to convert river waypoint data supplied in CE coordinates to TASC coordinates. Subroutine FIXLS is used to convert coastlines to the appropriate plotting coordinates.

Contours of constant time differences are computed using subroutine HYPER. Each contour is computed as the sequence of points, in TASC coordinates, which have the same Loran time difference. HYPER implements an iterative procedure using the RB model and starts with an initial point computed using a purely hyperbolic model. The contour values near the baseline are interpolated using a third-order spline fit in subroutine SPLNTRP.

Plotting is done using program AVCOPLOT. A simplified flow diagram is given in Fig. 8.2-1.

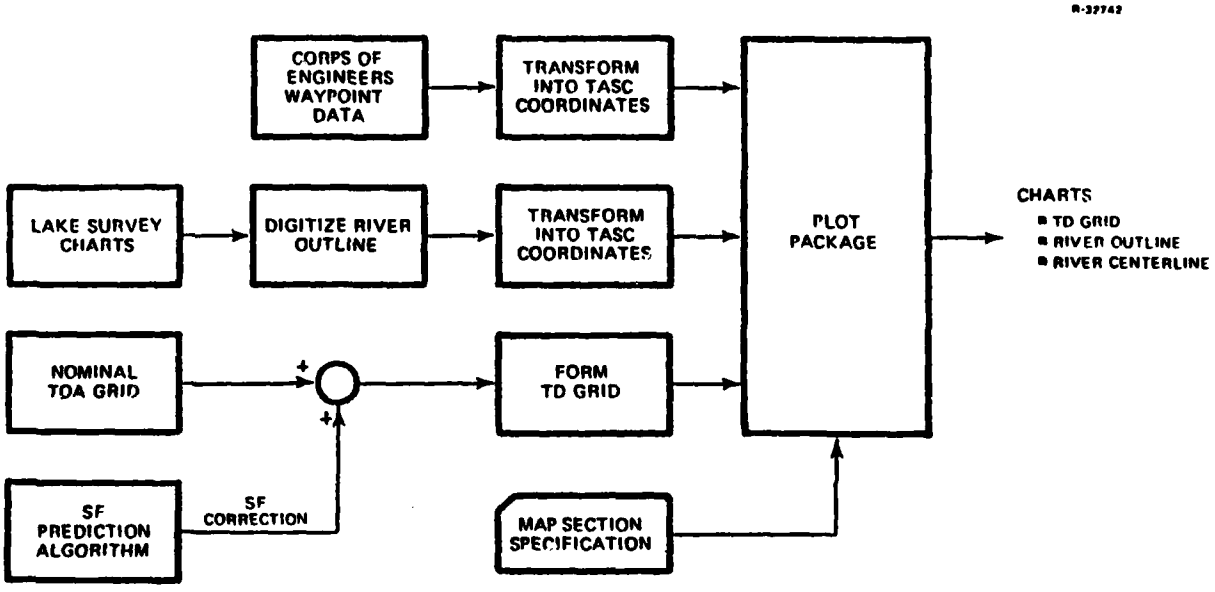

Figure 8.2-1 System Flow for St. Marys River Chart Predictions Software

8.3 ILLUSTRATIVE RESULTS

The actual drawings of the St. Marys River delivered as part of Task IIa of this effort are approximately 30 in x 42 in and cannot be reproduced in this report. Photographic reduction of the drawings would be illegible because of data density. An illustrative version of Lake Survey Chart No. 62 is shown in Fig. 8.3-1. Every tenth contour is plotted (the TD increment is 20 μsec). Channel centerlines are depicted by dashed lines and approximate coastlines are shown. Reference latitude and longitude marks are drawn in each corner and shown as a cross. The contours are labeled automatically by the plotting software (numbers have been enlarged for this drawing). Quantization error in the plotting software used to produce Fig. 8.3-1

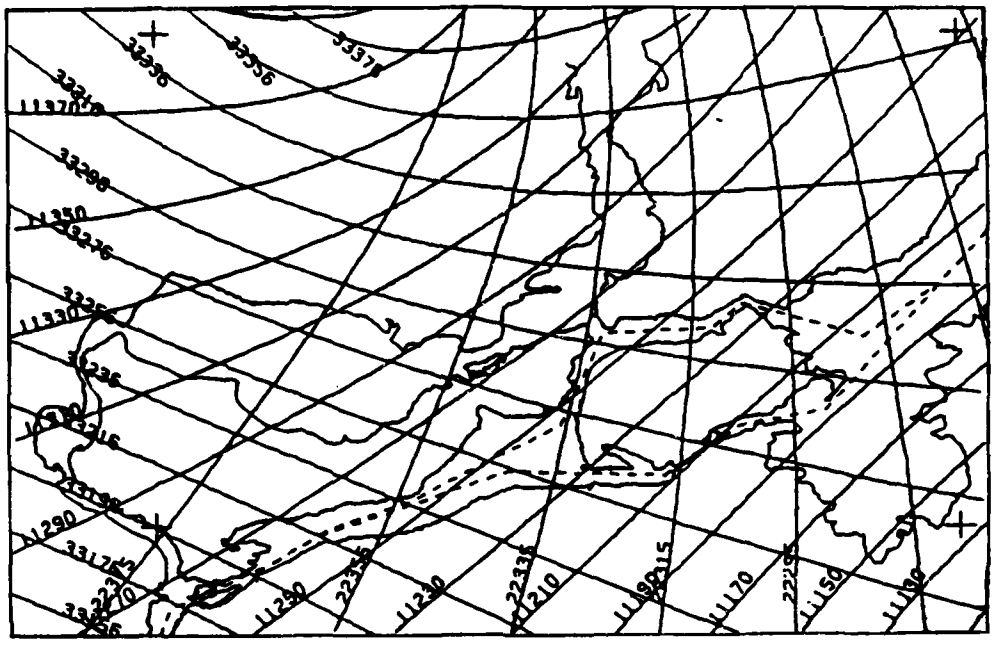

Figure 8.3-1 *Illustrative Drawing of Lake Survey Chart No. 62*

introduces an erroneous "wiggle" into the contours which is not present in the delivered charts.

During the chart production phase, it was discovered that the separation between the upbound and downbound channel centerlines for the Lime Island Channel are charted incorrectly on Lake Survey Chart No. 61. The actual separation is approximately one third of the distance shown on Lake Survey Chart No. 61.

9. SUMMARY, CONCLUSIONS AND RECOMMENDATIONS

9.1 SUMMARY

The specific objectives of this study were to develop a Loran-C time difference (TD) grid prediction model for the St. Marys River region and to use this model along with specifically gathered data to chart the area. The grid prediction methodology used is composed of:

- Data collection site selection
- On-line interaction with data collection team
- Semi-empirical grid prediction model development
- Data quality analysis
- Grid prediction model calibration
- Grid accuracy assessment
- Chart development.

Data collection site selection included: general considerations related to geophysical characteristics of the region, presurvey computer simulations to predict expected grid calibration accuracy with candidate sets of sites and development of prioritized lists of data collection sites. Considerable interaction with the Coast Guard Research and Development Center data collection team was required to establish a set of data collection sites which guaranteed the availability and accessibility of a sufficient number of sites at Corps of Engineers (CE) survey markers along the river. A total of 21 Priority 1 sites and 16

Priority 2 sites were specified by TASC. Loran-C data were actually collected at 23 sites which correspond quite closely to the specified Priority 1 sites.

The CE Horizontal Control System is a coordinate system, established by a first-order survey of the region, used to dredge the river channel and place the visual markers which establish the navigation waypoints (intersection of channel center line segments). Navigation satellite translocation was used to establish the location of additional sites (e.g., transmitter locations, sites along the river) relative to the WGS-72 reference ellipsoid. A weighted least-squares technique was applied to tie the two coordinate systems together with an estimated accuracy of approximately ± 10 ft. Accurate knowledge of all data collection site locations in a consistent coordinate system is an absolute necessity in any grid prediction technique.

Semi-empirical grid prediction models, which use theory to establish the functional form of a signal propagation delay model and a limited amount of data to calibrate the model formulations used, are intended to characterize the average spatial propagation delay characteristics over the entire region. The functional form of the model is capable of accounting for temporal variations in the Loran-C grid, providing temporal data are available to calibrate this portion of the model.

Data quality analysis is required to establish confidence in the data collection procedure, equipment performance and overall quality of the measurements prior to using these data to calibrate the grid prediction model parameters. Maverick data points were removed and the associated measurement errors identified to establish the expected bound on grid

prediction accuracy associated with the available data base. Overall quality of the TD data collected during the September/October 1977 data collection period is very high, with an estimated measurement error level of less than 20 nsec, 1σ.

Grid prediction model calibration is an interactive procedure whereby candidate models are fit to the data and the residual errors between the predicted and measured Loran-C TDs at each site are evaluated. The model which fits the data best yields the lowest residual errors. If the model fits the data exactly, the residual error will be on the order of the measurement error level determined from the data quality analysis. Of the several spatial models fit to the data base, the lowest residual error was achieved with a model which included both range dependence and bearing angle dependence. There is no firm theoretical basis for the bearing dependence other than that it accounts for changes in the average conductivity of a signal propagation path with bearing angle caused by varying amounts of land and water. After calibrating the range and bearing (RB)-dependent model, the residual rms time difference error over the ensemble of data collection sites is approximately 100 nsec, 1σ. This residual error is significantly larger than the estimated measurement error of 20 nsec and cannot be accounted for by a purely spatial propagation error model. Consequently, this residual grid prediction error must be attributed to local warpage of the Loran-C grid and/or temporal grid instability during the data collection period.

The exact contributions of local warpage errors and temporal grid instability to the total residual grid prediction error cannot be assessed from the available data. However, there is rather strong evidence that temporal grid instability may be a major source of this error. Analysis of User I and

User II TD data recorded at the waypoints during April 1976 and again during August 1976 yields a random error of roughly 180 nsec, 1σ, between the two time periods for the ensemble of waypoints. Additionally, data recorded during August, September/ October and November 1977, at the data collection sites under controlled conditions exhibits a temporal grid instability of roughly 100 nsec between these periods. This strongly suggests that fluctuations on the order of 100 nsec, 1σ, in the grid may occur over a time period of one month or less. Additional data are required to substantiate this observation and to model the phenomenon.

Chart production was the final step in the grid prediction effort. Three drawings of the St. Marys River region with the same size and scale of Lake Survey Chart Nos. 61, 62 and 63 were produced containing

- Latitude and longitude reference marks
- Approximate coastal outlines
- Channel centerlines
- Contours of constant Loran-C TDs.

During the charting effort, a suspected inconsistency in the Corps of Engineers grid was identified and explained along with discrepancies in the Lake Survey Charts. For example, the separation between the indicated upbound and downbound channel centerlines in the Lime Island Channel are incorrectly plotted on Lake Survey Chart No. 61. The Loran-C TD charts developed for the St. Marys River are separate deliverables and are not contained in this report.

9.2 CONCLUSIONS

The study objectives, to develop a Loran-C time difference prediction model for the St. Marys River region and to use this model along with specifically gathered data to chart the area, have been achieved. The specific grid calibration methodology used to achieve these objectives was demonstrated to be quite effective and is equally applicable to other short (and long) baseline Loran-C chains.

The data collection site selection procedure and associated data collection procedure yielded high quality measurement data with an estimated error level of less than 20 nsec/TD, 1σ. Satellite translocation provided accurate (9 ft, 1σ) position measurements at the Loran-C transmitters and data collection sites in a common coordinate system (WGS-72). Computer processing of the translocation data was used to establish the location of the navigation channel waypoints relative to the data collection sites with a computed error of less than 10 ft. An accurate reference system is an absolute necessity in any grid prediction procedure.

The calibrated semi-empirical grid prediction algorithm reduces the rms error between the measured and predicted TDs at the data collection sites from 350 nsec before algorithm calibration to 100 nsec after calibration. This residual error after calibration is considerably larger than the 20 nsec error level associated with the measurement data and cannot be accounted for with a spatial-area propagation model. Analysis of available data suggests that this residual error may be due to temporal grid instability. Variations in the measured TDs over a one- to two-month period have been observed to exceed 400 nsec at certain sites with a computed rms level of 100 nsec to 200 nsec. The contribution of local warpage

conditions to residual grid prediction error is not observable from the available data.

9.3 RECOMMENDATIONS

It is recommended that additional analytic studies be undertaken and long-term data collection efforts be initiated to determine the mechanism(s) for the apparent grid instability observed in the St. Marys River region. A quantitative evaluation of the residual error between the measured and predicted TDs with respect to meteorological parameters is required to assess the true impact of weather on Loran-C TDs in the St. Marys River region. These long-term data should also be used to calibrate temporal propagation parameters in the semi-empirical grid prediction algorithm.

In addition to the desire to improve St. Marys River chain performance through prediction and compensation of temporal effects, it is important to determine if this problem is fundamental to all short baseline Loran-C chains. Because temporal grid instability can be aggravated in portions of the coverage area by the present technique used by the SAM to control the chain, studies should also be initiated to assess the potential improvement in grid stability associated with utilizing multiple monitor sites and optimal data mixing for chain control.

APPENDIX A
CALIBRATED TD GRID PREDICTION ALGORITHMS

A.1 INTRODUCTION

Calibrated grid prediction algorithms are presented in this appendix for predicting the spatial-area TD component, $\overline{TD}$, at any user location. The spatial-area TD is the expected TD in the St. Marys River Loran-C signal coverage area based on the spatial-area average propagation properties of the coverage area during the September/October 1977, data collection time interval. The spatial-area TD is given by

$$\overline{TD}_{im} = (T_i - T_m) + \overline{SFTD}_{im} + \overline{ED}_i (\mu sec) \qquad (A.1)$$

where

$$T_i = \frac{nR_i}{c} (\mu sec)$$

$$T_m = \frac{nR_m}{c} (\mu sec)$$

R_i = i^{th} secondary station-to-user receiver path distance (ft)

R_m = master station-to-user receiver path distance (ft)

i = x, y or z secondary station

m = master station

c = speed of light in free space
= 983.5690892 (ft/μsec)

n = Refractive index of air = 1.000338

$\overline{ED}_x$ = 11221.652 (μsec)

$\overline{ED}_y$ = 22220.332 (μsec)

$\overline{ED}_z$ = 33227.934 (μsec)

$\overline{SFTD}_{im}$ = Differential spatial-area SF = $\overline{SF}_i - \overline{SF}_m$

$\overline{SF}$ = Spatial-area secondary phase factor* (SF)

The calibrated algorithm for predicting the differential spatial-area SF using the R model is given in Section A.2. The calibrated algorithm using the RB model is given in Section A.3. Both algorithms were calibrated using weighted measurement noise which is assumed to be 20 nsec/TD at the SAM site and scaled up with distance from the SAM site, with an average rms level of roughly 100 nsec/TD for the ensemble of sites.

A.2 RANGE(R)-DEPENDENT MODEL

The differential spatial-area SF for the R model is given by

$$\overline{SFTD}_{im} = \left(\frac{A_i}{T_i} + B_i T_i + C_i T_i^2\right) - \left(\frac{A_m}{T_m} + B_m T_m + C_m T_m^2\right) + b_{im} \text{ (μsec)} \qquad \text{(A.2-1)}$$

*Throughout this report, SF denotes the total secondary phase factor (or phase delay) of the groundwave signal propagating over any land and/or water path and not the SF associated with an equivalent length sea water path.

The calibrated coefficients for the R model are

$$
\begin{aligned}
A_x &= -68.19 && (\mu sec)^2 \\
B_x &= -0.006957 && (\mu sec/\mu sec) \\
C_x &= 0.00001475 && (\mu sec)^{-1} \\
A_y &= 119.9 && (\mu sec)^2 \\
B_y &= 0.02537 && (\mu sec/\mu sec) \\
C_y &= -0.00004459 && (\mu sec)^{-1} \\
A_z &= -11.72 && (\mu sec)^2 \\
B_z &= -0.001746 && (\mu sec/\mu sec) \\
C_z &= 0.000005959 && (\mu sec)^{-1} \\
A_m &= -165.4 && (\mu sec)^2 \\
B_m &= -0.01815 && (\mu sec/\mu sec) \\
C_m &= 0.00002688 && (\mu sec)^{-1} \\
b_{xm} &= -1.760 && (\mu sec) \\
b_{ym} &= -7.140 && (\mu sec) \\
b_{zm} &= -2.738 && (\mu sec)
\end{aligned}
\qquad \text{(A.2-2)}
$$

A.3 RANGE AND BEARING(RB)-DEPENDENT MODEL

The differential spatial-area SF for the RB model is given by

$$
\begin{aligned}
\overline{SFTD}_{im} = {} & A\left(\frac{1}{\overline{T}_i} - \frac{1}{\overline{T}_m}\right) + B\left(T_i - T_m\right) \\
& + T_i\left(C_i\overline{\beta}_i + D_i\overline{\beta}_i^{\,2}\right) - T_m\left(C_m\overline{\beta}_m + D_m\overline{\beta}_m^{\,2}\right) \\
& + b_{im} \quad (\mu sec)
\end{aligned}
\qquad \text{(A.3-1)}
$$

where $\bar{\beta}_i$ is the normalized data site path bearing angle, measured relative to a specific reference path direction chosen at the i^{th} station, and is defined as

$$\bar{\beta}_i = \frac{|\Delta\beta_i|}{|\beta_i(0)|} \qquad \text{(A.3-2)}$$

The reference direction for each station is defined by a unit vector at the station location with a bearing angle $\beta_i(0)$ measured from true north (clockwise rotation about the down vertical defines a positive bearing angle). The convention adopted for this model is to limit $\beta_i(0)$ to between -180 deg and +180 deg. The relative bearing angle, $\Delta\beta_i$, is defined as the included angle between the reference direction unit vector and a vector from the station location to the user position. For example, if the user is located in the reference direction from station i, $\Delta\beta_i$ is zero and the normalized bearing angle, $\bar{\beta}_i$, is zero. The magnitudes of $\Delta\beta_i$ and $\bar{\beta}_i$ increase for user locations on either side of the reference direction. The reference direction for each station is defined so that it roughly bisects the angular coverage area of the chain along the river:

$$\begin{aligned} \beta_x(0) &= 43.5(\text{deg}) \\ \beta_y(0) &= -64.0(\text{deg}) \\ \beta_z(0) &= -174.5(\text{deg}) \\ \beta_m(0) &= -133.4(\text{deg}) \end{aligned} \qquad \text{(A.3-3)}$$

The calibrated coefficients for the RB model are

$$
\begin{aligned}
A &= -15.40 && (\mu sec)^2 \\
B &= 0.002329 && (\mu sec/\mu sec) \\
C_x &= -0.005836 && (\mu sec/\mu sec) \\
C_y &= 0.002337 && (\mu sec/\mu sec) \\
C_z &= -0.01981 && (\mu sec/\mu sec) \\
C_m &= 0.0002885 && (\mu sec/\mu sec) \\
D_x &= 0.004633 && (\mu sec/\mu sec) \\
D_y &= -0.002841 && (\mu sec/\mu sec) \\
D_z &= 0.05834 && (\mu sec/\mu sec) \\
D_m &= -0.0001738 && (\mu sec/\mu sec) \\
b_{xm} &= 0.3758 && (\mu sec) \\
b_{ym} &= -0.4279 && (\mu sec) \\
b_{zm} &= 0.4168 && (\mu sec)
\end{aligned}
\qquad \text{(A.3-4)}
$$

A.4 REMARKS

Model coefficients presented in Sections A.2 and A.3 characterize the estimated spatial-area secondary phase factor ($\overline{SF}$) for the St. Marys River region during the September/October 1977, data collection period. It is important to note that these coefficients must be used in Eq. A.1-1 with the numerical values for emission delay ($\overline{ED}$), speed of light (c) and refractive index of air (n) specified herein. All of these parameter values form a consistent set of coefficients. For example, any difference between the actual ED used by the chain and the value specified herein has been absorbed by the TD bias term, b_{im}, through the calibration procedure.

APPENDIX B
TD GRID EVALUATION AT WAYPOINTS

This appendix presents the expected user position error and predicted TDs at the downbound and upbound river waypoints (see Fig. 1.1-1) obtained with the calibrated range and bearing(RB)-dependent model given in Appendix A. The north-east coordinates of the river waypoints, supplied to TASC by the Coast Guard, relative to the Army Corps of Engineers Triangle 19 are given in Table B.1. At each waypoint, the expected values of the following quantities are presented in this appendix:

- 2d rms user position error, associated with the XM-YM, YM-ZM and XM-ZM TD pairs, for an assumed user receiver noise of 10, 50 and 100 nsec/TD
- TDX, TDY and TDZ
- TD LOP gradients
- Crossing angles between TD LOPs.

B.2 USER POSITION FIX ERROR

In this section, the predicted user position fix error at each waypoint associated with the TD charts which were prepared using the RB grid prediction model algorithm (see Appendix A) is presented. A user position fix can be derived from any two of the three TDs at the user location.

TABLE B-1

ST. MARYS RIVER WAYPOINTS N-E COORDINATES (REFERENCED TO ARMY CORPS OF ENGINEERS MARKER - TRIANGLE 19)

WAYPOINT NAME		COORDINATES (ft)	
Old	New	North	East
1	A	7913.51759	-74132.21976
2	B	-18382.5868	-51064.5954
3	C	-13917.3241	-35537.0815
4	D	-12532.4097	-33276.7810
5	E	-8603.7343	-30928.6205
6	F	-858.5254	-20589.8726
7	H	1713.9831	-10199.5931
8	I	2147.1314	-140.1739
9	J	928.32	2058.62
10	K	-1077.8443	7868.3233
11	L	-16084.25	15508.98
12	M	-23523.7366	20587.5099
42	N	-25252.5357	21767.6662
43	O	-37536.6661	26360.3859
44	P	-60299.2170	39341.6768
45	Q	-66557.5173	55059.9715
46	R	-83210.8729	56107.0520
47	S	-87358.7552	60292.9136
13	T	-52707.3324	31498.5041
14	U	-76068.8391	30872.5384
15	V	-87330.3724	39297.2201
16	W	-100333.3351	41980.1441
48	X	-105937.8061	54709.11091
17	Y	-117311.806	63619.6553
18	Z	-130828.4701	80847.002
19	AA*	-135393.9341	82754.3819
64	BB	-151598.0494	80899.1513
20	CC	-155034.9993	80505.6503
63	DD	-155996.9988	83364.1807
21	EE	-164736.2021	101368.0586
62	FF	-171239.0399	115352.3922
22	GG	-178199.9993	112509.9999
23	HH	-184504.1337	113627.9755
24	II	-201664.1337	113627.9755

*The East coordinate of waypoint AA decreased 1000 ft by TASC to make it fall on the channel centerline.

The expected user TD error vector, $\delta\underline{z}_u^*$, associated with the charted TD LOP pair, used to compute a position fix, is given by

$$\delta\underline{z}_u^* = H_{td}\,\delta\hat{\underline{x}} + \underline{v}_g + \underline{v}_u \qquad \text{(B.2-1)}$$

where

$\delta\hat{\underline{x}}$ = error in the calibrated grid state vector, $\hat{\underline{x}}$

H_{td} = TD observation matrix at the user position

$\underline{v}_g$ = temporal TD grid instability vector at the user position

$\underline{v}_u$ = TD measurement noise (or receiver error) vector at the user position.

The user position error vector, $\delta\underline{x}_u$, is given by

$$\delta\underline{x}_u = H_u\delta\underline{z}_u^* \qquad \text{(B.2-2)}$$

where H_u is the TD error to position error vector transformation matrix. Substituting Eq. B.2-1 into B.2-2 gives

$$\delta\underline{x}_u = H_u\left[H_{td}\delta\hat{\underline{x}} + \underline{v}_g + \underline{v}_u\right] \qquad \text{(B.2-3)}$$

Therefore, the position error covariance matrix for the position fix grid lines is given by

$$P_{wp} = \text{Expected Value of } \{\delta\underline{x}_u\delta\underline{x}_u^T\}$$

or

$$\underbrace{P_{wp}}_{\substack{\text{Position}\\ \text{fix}\\ \text{Error}\\ \text{Covariance}}} = \underbrace{H_u\, H_{td}\, P_f(+)\, H_{td}^T H_u^T}_{\substack{\text{Spatial-Area}\\ \text{TD Grid Error}\\ \text{Covariance}}} + \underbrace{H_u\, R_g\, H_u^T}_{\substack{\text{Grid}\\ \text{Instability}\\ \text{Error}\\ \text{Covariance}}} + \underbrace{H_u\, R_u\, H_u^T}_{\substack{\text{User}\\ \text{Measurement}\\ \text{Noise Error}\\ \text{Covariance}}} \qquad \text{(B.2-4)}$$

where

$P_f(+)$ = calibrated grid model error covariance matrix (See Section 7.3)

R_u = user measurement noise error covariance matrix

R_g = TD Grid instability error covariance matrix.

The grid instability term is included in the computation of user position fix error to account for errors caused by expected temporal variations in the propagation properties of the medium from the average properties embodied in the calibrated grid prediction model. Grid instability errors are assumed to be of the same form and magnitude as those assumed during the calibration of the model (Section 7). Thus, lowest waypoint position errors are obtained if the grid instability errors are zero. The error covariance matrix, Eq. B.2-4, can be used to predict the expected position fix error for any Loran-C user utilizing the calibrated TD grid charts to obtain a position fix in the St. Marys River. The diagonal elements of the covariance matrix are the estimated variances of the position error along the north and east directions.

There are several ways to describe an expected position error at a user (or waypoint) location. These are:

- 2d rms (root-mean-square) position error
- Position error ellipse
- 2σ cross-channel position error

The 2d rms position error, as defined by the U.S. Coast Guard (Ref. 8), is

$$\text{2d rms error} = 2\sqrt{\sigma_N^2 + \sigma_E^2} \qquad \text{(B.2-5)}$$

where σ_N and σ_E, respectively, are the errors along north and east directions. The 2d rms error, as defined in Eq. B.2-5, is a scalar error based on one-dimensional error statistics.

A useful alternative pictorial representation of a two-dimensional position fix error* is by an error ellipse as illustrated in Fig. B.2-1 drawn for a given probability of occurrence of the position fix error. The dotted line through the ellipses connects the downbound waypoints. Waypoint error ellipses are drawn for the St. Marys River TD grid with no assumed grid instability (see Fig. 7.5-1) with the error ellipse major axis equal to the 2d rms waypoint error. Thus, the area within each of these error ellipses shows the region within which the computed waypoint position will lie with a probability of 85% (Ref. 9). The ellipse provides a visual display of both the cross-channel and along-channel errors for the given error probability. Another desirable error presentation is in terms of the expected 2σ cross-channel error (see Fig. 7.5-2). The cross-channel error is of special interest to a user navigating a straight and narrow channel.

*Fix errors are assumed to be described by a two-dimensional Gaussian error statistic (Ref. 9).

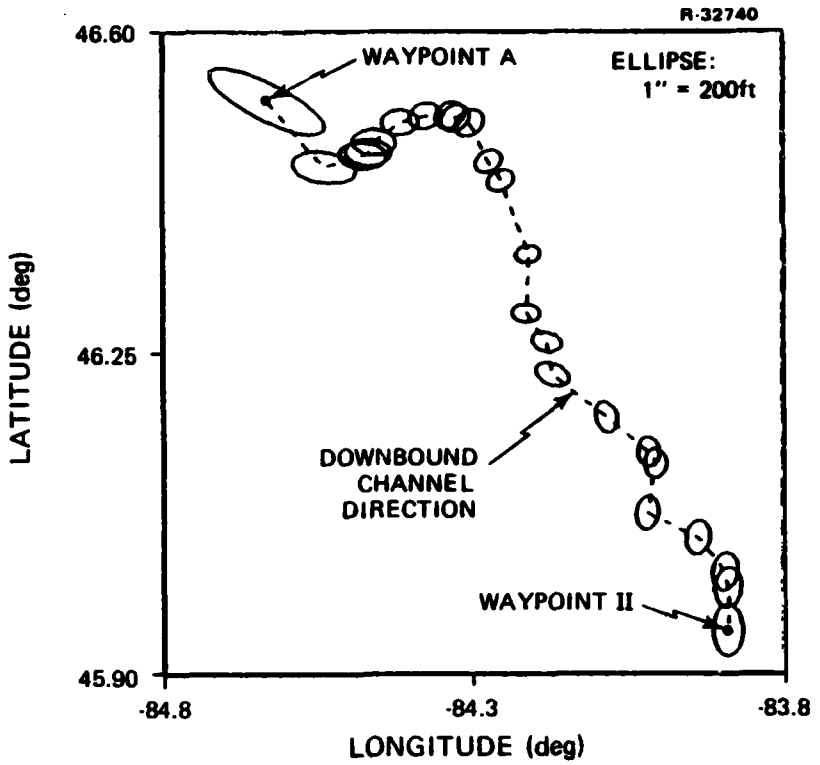

Figure B.2-1 Illustration Waypoint Error Ellipses

Tables B.2-1 through B.2-12 give the predicted 2d rms user position error using the MX-MY, MY-MZ and MX-MZ station combinations at the downbound and upbound waypoints for an assumed user TD measurement (1σ) noise of 10, 50 and 100 nsec. Tables B.2-1 through B.2-6 present the expected 2d rms position errors with the assumed TD grid instability, while Tables B.2-7 through B.2-12 give errors without the assumed TD grid instability. These tables also show the expected minimum position error at each waypoint along with the associated combination of transmitter stations that yields this minimum error.

B.3 WAYPOINT GRID DATA

This section presents the predicted Loran-C TDs, gradient of the TD LOPs and crossing angles between LOPs

at downbound and upbound waypoints in the St. Marys River. Tables B.3-1 and B.3-2 give the TDs at the downbound and upbound waypoints, respectively, as predicted by the calibrated St. Marys TD grid prediction model. Note, these TDs are the spatial-area TDs based on average propagation properties that existed during the model calibration time interval.

The gradient of a TD LOP, $\underline{\nabla}$, is a vector that relates the TD error to position error. Its direction is normal to the TD LOP and its magnitude is given by

$$|\underline{\nabla}| = \frac{2}{c} \text{Sin} \frac{\psi}{2} \left(\frac{\text{nsec}}{\text{ft}}\right) \qquad \text{(B.3-1)}$$

where c is the speed of light (ft/nsec); and ψ is the angle (see Fig. B.3-1) between the path bearings to the secondary and master stations. Tables B.3-3 and B.3-4 present the expected sensitivity (i.e., gradient-inverse), in ft/nsec, of the predicted TD LOPs at the downbound and upbound waypoints of the river, respectively. These tables also show the crossing angle, θ, between various LOPs at each of the river waypoints.

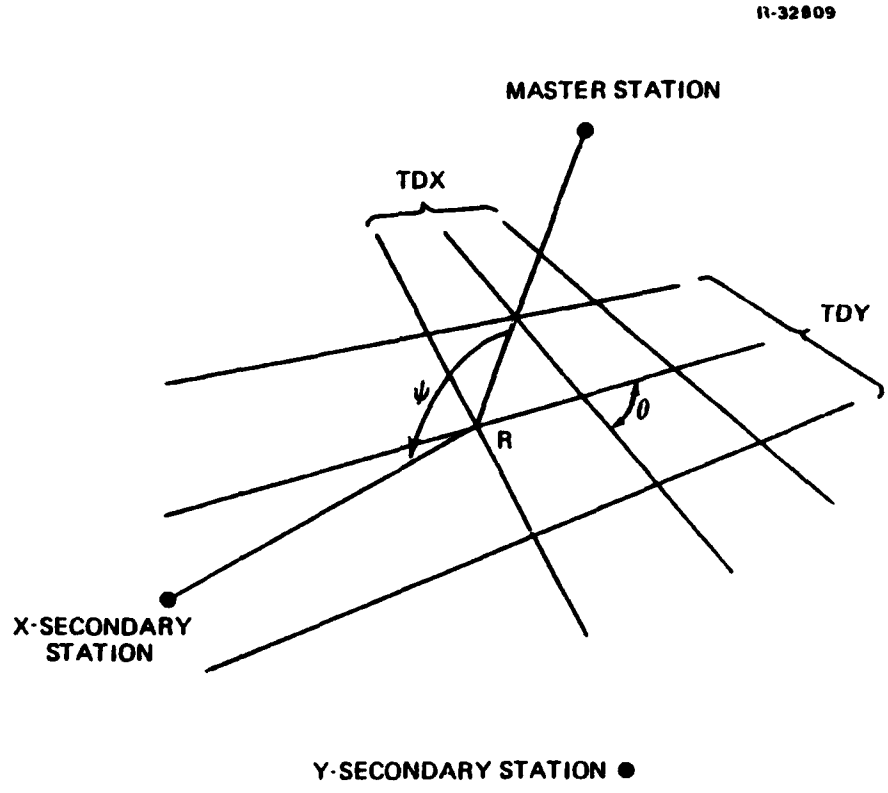

Figure B.3-1 Definition of Included Path Bearing Angle (ψ) and Crossing Angle (θ)

TABLE B.2-1

PREDICTED USER 2d RMS POSITION ERROR AT DOWNBOUND WAYPOINTS
WITH ASSUMED GRID INSTABILITY
(USER MEASUREMENT ERROR = 10 nsec, 1σ)

Waypoint	2d RMS Position Error (ft)				
	MXY	MYZ	MXZ	Minimum Error	Minimum Error Stations
A	870	1000	700	700	MXZ
B	550	437	330	330	MXZ
C	365	302	231	231	MXZ
D	338	284	219	219	MXZ
E	325	272	211	211	MXZ
F	276	215	173	173	MXZ
H	223	161	134	134	MXZ
I	200	120	103	103	MXZ
J	192	110	94	94	MXZ
K	179	92	78	78	MXZ
L	128	59	42	42	MXZ
M	112	63	53	53	MXZ
T	92	130	151	92	MXY
U	131	180	232	131	MXY
V	143	227	304	143	MXY
W	175	269	380	175	MXY
Y	199	371	608	199	MXY
Z	235	475	883	235	MXY
AA	252	498	959	252	MXY
CC	339	525	1226	339	MXY
EE	372	652	1659	372	MXY
GG	442	737	2117	442	MXY
HH	488	756	2299	488	MXY
II	648	807	2836	648	MXY

TABLE B.2-2

PREDICTED USER 2d RMS POSITION ERROR AT UPBOUND WAYPOINTS
WITH ASSUMED GRID INSTABILITY
(USER MEASUREMENT ERROR = 10 nsec, 1σ)

Waypoint	2d RMS Position Error (ft)				
	MXY	MYZ	MXZ	Minimum Error	Minimum Error Stations
A	870	1000	700	700	MXZ
B	550	437	330	330	MXZ
C	365	302	231	231	MXZ
D	338	284	219	219	MXZ
E	325	272	211	211	MXZ
F	276	215	173	173	MXZ
H	223	161	134	134	MXZ
I	200	120	103	103	MXZ
J	192	110	94	94	MXZ
K	179	92	78	78	MXZ
L	128	59	42	42	MXZ
M	112	63	53	53	MXZ
N	120	68	55	55	MXZ
O	104	92	93	92	MYZ
P	98	165	195	98	MXY
Q	113	229	273	113	MXY
R	129	268	351	129	MXY
S	138	294	393	138	MXY
X	173	315	471	173	MXY
Y	199	371	608	199	MXY
Z	235	475	883	235	MXY
AA	252	498	959	252	MXY
BB	326	523	1171	326	MXY
DD	341	540	1275	341	MXY
FF	561	750	2229	561	MXY
II	648	807	2836	648	MXY

TABLE B.2-3

PREDICTED USER 2d RMS POSITION ERROR AT DOWNBOUND WAYPOINTS
WITH ASSUMED GRID INSTABILITY
(USER MEASUREMENT ERROR = 50 nsec, 1σ)

Waypoint	2d RMS Position Error (ft)				
	MXY	MYZ	MXZ	Minimum Error	Minimum Error Stations
A	1267	1062	723	723	MXZ
B	844	490	350	350	MXZ
C	675	360	253	253	MXZ
D	656	344	242	242	MXZ
E	655	334	235	235	MXZ
F	626	287	199	199	MXZ
H	583	246	167	167	MXZ
I	548	219	144	144	MXZ
J	533	212	137	137	MXZ
K	503	200	127	127	MXZ
L	393	165	103	103	MXZ
M	345	157	106	106	MXZ
T	230	174	176	174	MYZ
U	213	213	251	213	MXY
V	200	252	321	200	MXY
W	215	291	396	215	MXY
Y	222	388	626	222	MXY
Z	251	491	905	251	MXY
AA	268	514	982	268	MXY
CC	351	544	1254	351	MXY
EE	383	671	1694	383	MXY
GG	452	758	2161	452	MXY
HH	498	779	2347	498	MXY
II	658	835	2893	658	MXY

TABLE B.2-4

PREDICTED USER 2d RMS POSITION ERROR AT UPBOUND WAYPOINTS
WITH ASSUMED GRID INSTABILITY
(USER MEASUREMENT ERROR = 50 nsec, 1σ)

Waypoint	2d RMS Position Error (ft)				
	MXY	MYZ	MXZ	Minimum Error	Minimum Error Stations
A	1267	1062	723	723	MXZ
B	844	490	350	350	MXZ
C	675	360	253	253	MXZ
D	656	344	242	242	MXZ
E	655	334	235	235	MXZ
F	626	287	199	199	MXZ
H	583	246	167	167	MXZ
I	548	219	144	144	MXZ
J	533	212	137	137	MXZ
K	503	200	127	127	MXZ
L	393	165	103	103	MXZ
M	345	157	106	106	MXZ
N	338	157	107	107	MXZ
O	282	157	130	130	MXZ
P	206	198	216	198	MYZ
Q	187	250	290	187	MXY
R	181	287	367	181	MXY
S	183	311	410	183	MXY
X	205	333	487	205	MXY
Y	222	388	626	222	MXY
Z	251	491	905	251	MXY
AA	268	514	982	268	MXY
BB	338	541	1198	338	MXY
DD	353	559	1303	353	MXY
FF	568	769	2266	568	MXY
II	658	835	2893	658	MXY

TABLE B.2-5

PREDICTED USER 2d RMS POSITION ERROR AT DOWNBOUND WAYPOINTS
WITH ASSUMED GRID INSTABILITY
(USER MEASUREMENT ERROR = 100 nsec, 1σ)

Waypoint	2d RMS Position Error (ft)				
	MXY	MYZ	MXZ	Minimum Error	Minimum Error Stations
A	2063	1237	790	790	MXZ
B	1413	627	408	408	MXZ
C	1210	501	314	314	MXZ
D	1191	487	303	303	MXZ
E	1200	480	296	296	MXZ
F	1175	442	266	266	MXZ
H	1116	411	242	242	MXZ
I	1055	392	228	228	MXZ
J	1027	385	224	224	MXZ
K	971	372	217	217	MXZ
L	765	318	196	196	MXZ
M	672	298	195	195	MXZ
T	437	270	237	237	MXZ
U	364	292	301	292	MYZ
V	319	318	367	318	MYZ
W	307	353	441	307	MXY
Y	282	438	678	282	MXY
Z	298	537	969	298	MXY
AA	311	560	1049	311	MXY
CC	385	600	1335	385	MXY
EE	415	726	1800	415	MXY
GG	482	819	2292	482	MXY
HH	527	844	2488	527	MXY
II	686	915	3063	686	MXY

TABLE B.2-6

PREDICTED USER 2d RMS POSITION ERROR AT UPBOUND WAYPOINTS
WITH ASSUMED GRID INSTABILITY
(USER MEASUREMENT ERROR = 100 nsec, 1σ)

Waypoint	2d RMS Position Error (ft)				
	MXY	MYZ	MXZ	Minimum Error	Minimum Error Stations
A	2063	1237	790	790	MXZ
B	1413	627	408	408	MXZ
C	1210	501	314	314	MXZ
D	1191	487	303	303	MXZ
E	1200	480	296	296	MXZ
F	1175	442	266	266	MXZ
H	1116	411	242	242	MXZ
I	1055	392	228	228	MXZ
J	1027	385	224	224	MXZ
K	971	372	217	217	MXZ
L	765	318	196	196	MXZ
M	672	298	195	195	MXZ
N	654	295	195	195	MXZ
O	543	275	205	205	MXZ
P	380	277	271	271	MXZ
Q	323	307	340	307	MYZ
R	289	339	414	289	MXY
S	280	359	456	280	MXY
X	282	386	534	282	MXY
Y	282	438	678	282	MXY
Z	298	537	969	298	MXY
AA	311	560	1049	311	MXY
BB	373	595	1277	373	MXY
DD	387	614	1387	387	MXY
FF	592	826	2380	592	MXY
II	686	915	3063	686	MXY

TABLE B.2-7

PREDICTED USER 2d RMS POSITION ERROR AT DOWNBOUND WAYPOINTS
WITHOUT ASSUMED GRID INSTABILITY
(USER MEASUREMENT ERROR = 10 nsec, 1σ)

Waypoint	2d RMS Position Error (ft)				
	MXY	MYZ	MXZ	Minimum Error	Minimum Error Stations
A	750	322	184	184	MXZ
B	489	188	107	107	MXZ
C	314	129	81	81	MXZ
D	294	122	78	78	MXZ
E	274	116	78	78	MXZ
F	221	103	78	78	MXZ
H	186	86	64	64	MXZ
I	165	71	49	49	MXZ
J	159	67	45	45	MXZ
K	150	62	39	39	MXZ
L	112	49	31	31	MXZ
M	98	46	31	31	MXZ
T	74	49	39	39	MXZ
U	81	60	54	54	MXZ
V	74	70	66	66	MXZ
W	84	93	88	84	MXY
Y	69	95	119	69	MXY
Z	69	123	186	69	MXY
AA	74	133	206	74	MXY
CC	90	169	284	90	MXY
EE	87	212	426	87	MXY
GG	89	262	597	89	MXY
HH	97	282	663	97	MXY
II	139	358	869	139	MXY

TABLE B.2-8

PREDICTED USER 2d RMS POSITION ERROR AT UPBOUND WAYPOINTS
WITHOUT ASSUMED GRID INSTABILITY
(USER MEASUREMENT ERROR = 10 nsec, 1σ)

Waypoint	2d RMS Position Error (ft)				
	MXY	MYZ	MXZ	Minimum Error	Minimum Error Stations
A	750	322	184	184	MXZ
B	489	188	107	107	MXZ
C	314	129	81	81	MXZ
D	294	122	78	78	MXZ
E	274	116	78	78	MXZ
F	221	103	78	78	MXZ
H	186	86	64	64	MXZ
I	165	71	49	49	MXZ
J	159	67	45	45	MXZ
K	150	62	39	39	MXZ
L	112	49	31	31	MXZ
M	98	46	31	31	MXZ
N	96	46	32	32	MXZ
O	83	46	34	34	MXZ
P	70	52	45	45	MXZ
Q	80	68	69	68	MYZ
R	77	76	80	76	MYZ
S	83	85	95	83	MXY
X	68	88	97	68	MXY
Y	69	95	119	69	MXY
Z	69	123	186	69	MXY
AA	74	133	206	74	MXY
BB	98	168	267	98	MXY
DD	90	174	298	90	MXY
FF	87	254	563	87	MXY
II	139	358	869	139	MXY

TABLE B.2-9

PREDICTED USER 2d RMS POSITION ERROR AT DOWNBOUND WAYPOINTS
WITHOUT ASSUMED GRID INSTABILITY
(USER MEASUREMENT ERROR = 50 nsec, 1σ)

Waypoint	2d RMS Position Error (ft)				
	MXY	MYZ	MXZ	Minimum Error	Minimum Error Stations
A	1188	482	258	258	MXZ
B	806	290	160	160	MXZ
C	649	236	132	132	MXZ
D	635	230	129	129	MXZ
E	631	227	129	129	MXZ
F	604	216	126	126	MXZ
H	570	205	118	118	MXZ
I	536	197	111	111	MXZ
J	522	194	109	109	MXZ
K	493	188	107	107	MXZ
L	387	162	99	99	MXZ
M	341	151	98	98	MXZ
T	223	126	98	98	MXZ
U	186	128	109	109	MXZ
V	159	130	121	121	MXZ
W	149	146	141	141	MXZ
Y	120	149	190	120	MXY
Z	114	174	271	114	MXY
AA	116	184	295	116	MXY
CC	127	221	385	127	MXY
EE	126	264	547	126	MXY
GG	130	316	737	130	MXY
HH	138	338	811	138	MXY
II	178	416	1039	178	MXY

TABLE B.2-10

PREDICTED USER 2d RMS POSITION ERROR AT UPBOUND WAYPOINTS
WITHOUT ASSUMED GRID INSTABILITY
(USER MEASUREMENT ERROR = 50 nsec, 1σ)

Waypoint	2d RMS Position Error (ft)				
	MXY	MYZ	MXZ	Minimum Error	Minimum Error Stations
A	1188	482	258	258	MXZ
B	806	290	160	160	MXZ
C	649	236	132	132	MXZ
D	635	230	129	129	MXZ
E	631	227	129	129	MXZ
F	604	216	126	126	MXZ
H	570	205	118	118	MXZ
I	536	197	111	111	MXZ
J	522	194	109	109	MXZ
K	493	188	107	107	MXZ
L	387	162	99	99	MXZ
M	341	151	98	98	MXZ
N	331	148	97	97	MXZ
O	275	136	96	96	MXZ
P	194	121	103	103	MXZ
Q	169	122	121	121	MXZ
R	149	127	135	127	MYZ
S	146	133	148	133	MYZ
X	129	141	158	129	MXY
Y	120	149	190	120	MXY
Z	114	174	271	114	MXY
AA	116	184	295	116	MXY
BB	133	219	366	133	MXY
DD	127	225	401	127	MXY
FF	128	306	697	128	MXY
II	178	416	1039	178	MXY

TABLE B.2-11

PREDICTED USER 2d RMS POSITION ERROR AT DOWNBOUND WAYPOINTS
WITHOUT ASSUMED GRID INSTABILITY
(USER MEASUREMENT ERROR = 100 nsec, 1σ)

Waypoint	2d RMS Position Error (ft)				
	MXY	MYZ	MXZ	Minimum Error	Minimum Error Stations
A	2015	795	411	411	MXZ
B	1390	487	263	263	MXZ
C	1195	420	227	227	MXZ
D	1179	414	224	224	MXZ
E	1187	412	222	222	MXZ
F	1163	400	216	216	MXZ
H	1109	388	211	211	MXZ
I	1049	380	209	209	MXZ
J	1021	375	208	208	MXZ
K	966	366	207	207	MXZ
L	762	317	194	194	MXZ
M	670	295	190	190	MXZ
T	434	242	187	187	MXZ
U	350	237	199	199	MXZ
V	295	234	216	216	MXZ
W	265	247	241	241	MXZ
Y	212	251	322	212	MXY
Z	196	279	441	196	MXY
AA	196	290	474	196	MXY
CC	204	335	600	204	MXY
EE	204	383	816	204	MXY
GG	213	444	1063	213	MXY
HH	222	470	1159	222	MXY
II	265	561	1446	265	MXY

TABLE B.2-12

PREDICTED USER 2d RMS POSITION ERROR AT UPBOUND WAYPOINTS
WITHOUT ASSUMED GRID INSTABILITY
(USER MEASUREMENT ERROR = 100 nsec, 1σ)

Waypoint	2d RMS Position Error (ft)				
	MXY	MYZ	MXZ	Minimum Error	Minimum Error Stations
A	2015	795	411	411	MXZ
B	1390	487	263	263	MXZ
C	1195	420	227	227	MXZ
D	1179	414	224	224	MXZ
E	1187	412	222	222	MXZ
F	1163	400	216	216	MXZ
H	1109	388	211	211	MXZ
I	1049	380	209	209	MXZ
J	1021	375	208	208	MXZ
K	966	366	207	207	MXZ
L	762	317	194	194	MXZ
M	670	295	190	190	MXZ
N	650	290	190	190	MXZ
O	539	264	186	186	MXZ
P	374	229	193	193	MXZ
Q	313	216	214	214	MXZ
R	270	221	234	221	MYZ
S	257	224	250	224	MYZ
X	232	241	271	232	MXY
Y	212	251	322	212	MXY
Z	196	279	441	196	MXY
AA	196	290	474	196	MXY
BB	206	329	574	206	MXY
DD	203	340	623	203	MXY
FF	208	429	1007	208	MXY
II	265	561	1446	265	MXY

TABLE B.3-1

PREDICTED TIME DIFFERENCE AT DOWNBOUND WAYPOINTS

Waypoint	Time Difference - TD (μsec)		
	TDX	TDY	TDZ
A	11204.071	22353.977	33079.161
B	11197.707	22346.031	33117.836
C	11213.252	22351.868	33126.782
D	11216.292	22353.145	33127.550
E	11221.607	22355.785	33125.530
F	11236.910	22362.321	33129.016
H	11248.528	22366.377	33141.101
I	11258.760	22369.454	33156.839
J	11260.106	22369.522	33161.780
K	11264.716	22370.298	33173.671
L	11261.288	22364.571	33200.998
M	11260.747	22361.529	33216.166
T	11243.967	22341.501	33255.436
U	11212.807	22317.421	33266.325
V	11208.351	22305.082	33282.065
W	11193.225	22288.965	33288.852
Y	11200.148	22262.198	33316.177
Z	11206.379	22235.574	33332.956
AA	11203.289	22227.718	33334.189
CC	11178.504	22200.820	33330.113
EE	11194.916	22172.248	33344.694
GG	11195.223	22144.361	33349.697
HH	11191.261	22135.433	33349.279
II	11178.885	22116.891	33346.498

TABLE B.3-2

PREDICTED TIME DIFFERENCE AT UPBOUND WAYPOINTS

Waypoint	Time Difference - TD (μsec)		
	TDX	TDY	TDZ
A	11204.071	22353.977	33079.161
B	11197.707	22346.031	33117.836
C	11213.252	22351.868	33126.782
D	11216.292	22353.145	33127.550
E	11221.607	22355.785	33125.530
F	11236.910	22362.321	33129.016
H	11248.528	22366.377	33141.101
I	11258.760	22369.454	33156.839
J	11260.106	22369.522	33161.780
K	11264.716	22370.298	33173.671
L	11261.288	22364.571	33200.998
M	11260.747	22361.529	33216.166
N	11260.595	22360.755	33219.623
O	11254.245	22353.197	33237.006
P	11245.330	22335.847	33271.879
Q	11259.780	22332.055	33298.923
R	11238.218	22310.850	33304.255
S	11238.332	22305.256	33310.603
X	11203.348	22280.122	33305.380
Y	11200.148	22262.198	33316.177
Z	11206.379	22235.574	33332.956
AA	11203.289	22227.718	33334.189
BB	11182.536	22205.302	33330.785
DD	11181.294	22197.644	33332.345
FF	11204.243	22151.011	33352.731
II	11178.885	22116.891	33346.498

TABLE B.3-3

GRADIENT AND LOP CROSSING ANGLE AT DOWNBOUND WAYPOINTS

Waypoint	(Gradient)$^{-1}$=Sensitivity (ft/ns)			LOP Crossing Angle (deg)		
	ΔTDX	ΔTDY	ΔTDZ	MXY	MYZ	MXZ
A	1.05	2.11	1.10	14.5	40.4	54.9
B	0.87	1.74	0.76	17.3	56.9	74.2
C	0.84	1.72	0.65	19.2	65.4	84.5
D	0.84	1.72	0.64	19.4	66.8	86.2
E	0.84	1.76	0.62	19.5	68.7	88.2
F	0.84	1.82	0.56	20.3	77.0	82.7
H	0.82	1.83	0.53	21.3	84.4	74.4
I	0.80	1.82	0.51	22.3	89.8	67.9
J	0.79	1.80	0.51	22.6	89.7	67.1
K	0.77	1.75	0.51	23.4	88.0	64.7
L	0.70	1.50	0.52	25.6	89.5	64.9
M	0.66	1.38	0.53	27.1	88.9	64.0
T	0.56	1.03	0.59	32.9	84.6	62.4
U	0.52	0.91	0.67	37.8	79.1	63.1
V	0.50	0.83	0.72	42.6	78.9	58.5
W	0.49	0.80	0.79	47.6	76.7	55.7
Y	0.51	0.69	0.91	57.9	78.0	44.1
Z	0.55	0.63	1.06	64.8	78.6	36.6
AA	0.56	0.62	1.10	67.0	77.8	35.2
CC	0.60	0.66	1.21	77.8	71.6	30.6
EE	0.67	0.62	1.40	80.9	72.7	26.3
GG	0.74	0.62	1.57	87.3	69.6	23.1
HH	0.77	0.64	1.61	89.0	67.0	22.0
II	0.84	0.72	1.71	78.1	59.0	19.1

TABLE B.3-4

GRADIENT AND LOP CROSSING ANGLE AT UPBOUND WAYPOINTS

Waypoint	(Gradient)$^{-1}$=Sensitivity (ft/ns)			LOP Crossing Angle (deg)		
	ΔTDX	ΔTDY	ΔTDZ	MXY	MYZ	MXZ
A	1.05	2.11	1.10	14.5	40.4	54.9
B	0.87	1.74	0.76	17.3	56.9	74.2
C	0.84	1.72	0.65	19.2	65.4	84.5
D	0.84	1.72	0.64	19.4	66.8	86.2
E	0.84	1.76	0.62	19.5	68.7	88.2
F	0.84	1.82	0.56	20.3	77.0	82.7
H	0.82	1.83	0.53	21.3	84.4	74.4
I	0.80	1.82	0.51	22.3	89.8	67.9
J	0.79	1.80	0.51	22.6	89.7	67.1
K	0.77	1.75	0.51	23.4	88.0	64.7
L	0.70	1.50	0.52	25.6	89.5	64.9
M	0.66	1.38	0.53	27.1	88.9	64.0
N	0.66	1.35	0.53	27.4	88.8	63.7
O	0.61	1.19	0.55	29.7	86.9	63.4
P	0.53	0.94	0.61	35.6	85.1	59.3
Q	0.51	0.82	0.63	39.0	87.9	53.1
R	0.49	0.75	0.71	43.8	84.2	51.9
S	0.49	0.72	0.74	45.6	84.3	50.0
X	0.49	0.73	0.83	52.0	78.6	49.5
Y	0.51	0.69	0.91	57.9	78.0	44.1
Z	0.55	0.63	1.06	64.8	78.6	36.6
AA	0.56	0.62	1.10	67.0	77.8	35.2
BB	0.59	0.65	1.19	75.9	72.7	31.5
DD	0.61	0.65	1.23	78.1	71.9	30.0
FF	0.72	0.60	1.56	82.6	73.3	24.1
II	0.84	0.72	1.71	78.1	59.0	19.1

REFERENCES

1. Johler, J.R., Keller, W.J. and Walters, L.C., "Phase of the Low Radio Frequency Ground Wave," National Bureau of Standards Circular 573, June 1956.

2. Wait, J.R. and Walters, L.C., "Curves for Ground Wave Propagation over Mixed Land and Sea Paths," IEEE Transactions on Antennas and Propagation," Vol. AP-11, January 1963.

3. Hufford, G.A., "An Integral Equation Approach to the Problem of Wave Propagation over an Irregular Surface," Quarterly Journal of Applied Math, Vol. 9, No. 4, 1952.

4. Millington, G., "Ground Wave Propagation over an Inhomogeneous Smooth Earth," Proceedings of the Institute of Electrical Engineers, Vol. 96, Pt. III, January 1949.

5. Wait, J.R., "Recent Analytical Investigations of Electromagnetic Ground Wave Propagation over Inhomogeneous Earth Models," Proceedings of the IEEE, Vol. 62, No. 8, August 1974.

6. Gupta, R.R., "Groundwave Signal Prediction Techniques," The Analytic Sciences Corporation, Technical Information Memorandum TIM-735-3, July 1976.

7. Gelb, A. (Ed.), Applied Optimal Estimation, The MIT Press, Cambridge, Massachusetts, 1974.

8. Shubbuck, T.J., "St. Marys River Loran-C Evaluation," U.S. Coast Guard Research and Development Center, Interim Report No. 2, 30 November 1976.

9. Van Trees, H.L., Detection, Estimation and Modulation Theory, Part I, John Wiley and Sons, Inc., New York, 1968.

10. Hemmelblau, D.M., Process Analysis by Statistical Methods, John Wiley and Sons, Inc., New York, 1968.

REFERENCES (Continued)

11. Department of Defense, "World Geodetic System 1972," (U), DMA Technical Report 0002, January 1974 (CONFIDENTIAL).

12. Weir, J., Personal Communication with R. Healy, 29 August 1977.

13. "Correction Due to Error of Orientation of Δ19 System," Unpublished Memorandum, undated.

* U.S.G.P.O. 625-790/1302-2006

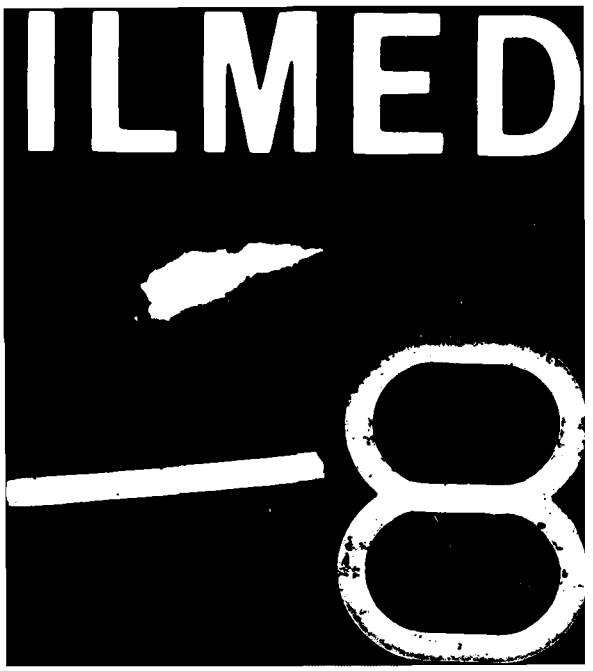
ILMED
8